

## **Bisindenoisoquinoline NSC 727357, a DNA intercalator and topoisomerase inhibitor with antitumor activity**

**SMITHA ANTONY, KELI K AGAMA, ZE-HONG MIAO, MELINDA HOLLINGSHEAD, SUSAN L. HOLBECK, MOLLIE H WRIGHT, LYUBA VARTICOVSKI, MUTHUKAMAN NAGARAJAN, ANDREW MORRELL, MARK CUSHMAN AND YVES POMMIER**

*Laboratory of Molecular Pharmacology (S.A., K.K.A., Z-H.M., Y.P.), Biological Testing Branch (M.H.), Developmental Therapeutics Program, Information Technology Branch (S.L.H.), Laboratory of Human Carcinogenesis (M.H.W., L.V.), National Cancer Institute, National Institutes of Health, Bethesda, Maryland 20892-4255, and Department of Medicinal Chemistry and Molecular Pharmacology, Purdue University, West Lafayette, Indiana 47907-1333 (M.N., A.M., M.C.)*

Running title: Topoisomerase I inhibition by NSC 727357

Corresponding Author: Yves Pommier

Laboratory of Molecular Pharmacology,

Center for Cancer Research, National Cancer Institute,

37 Convent Drive, Bldg 37, Room 5068, National Institutes of Health

Bethesda, Maryland, USA 20892-4255

Phone: 301-496-5944

Fax: 301-402-0752

Email: [pommier@nih.gov](mailto:pommier@nih.gov)

Number of text pages: 41

Number of tables: 0

Number of Figures: 11

Number of references: 49

Number of words in the Abstract: 164

Number of words in the Introduction: 570

Number of words in the Discussion: 898

**ABBREVIATIONS:** NSC 314622, 5,6-dihydro-5,11-diketo-2,3-dimethoxy-6-methyl-8,9-methylenedioxy-11H-indeno(1,2-c)isoquinoline; NSC 725671, 5,6-dihydro-5,11-dioxo-5-(3-amino-propyl)-11H-indeno(1,2-c)isoquinoline hydrochloride; NSC 727357, bis-1,3-((5,6-dihydro-5,11-diketo-11H-indeno[1,2-c]isoquinoline)-6-propylamino)propane bis(trifluoroacetate).

## ABSTRACT

Indenoisoquinolines are topoisomerase I (Top1) inhibitors developed to overcome some of the limitations of camptothecins and expand their anticancer spectrum. NSC 727357 is a novel dimeric indenoisoquinoline derivative with potent antiproliferative activity in the NCI-60 cell line panel, promising hollow fiber activity (score = 32) and activity against xenografts. Submicromolar concentrations of the bisindenoisoquinoline NSC 727357 induce Top1 cleavage complexes at specific sites in biochemical assays. At higher concentrations an inhibition of Top1 catalytic activity and DNA intercalation are observed. NSC 727357 also induces a limited number of Top2-DNA cleavage complexes. In contrast to the effect of other Top1 inhibitors, cells treated with the bisindenoisoquinoline NSC 727357 show an arrest of cell cycle progression in G1 with no significant inhibition of DNA synthesis following a short exposure to the drug. Moreover, unlike camptothecin and the indenoisoquinoline MJ-III-65 (NSC 706744), the cytotoxicity of bisindenoisoquinoline NSC 727357 is only partially dependent on Top1 and p53, indicating that this drug has additional targets besides Top1 and Top2.

## INTRODUCTION

Camptothecin (CPT) and its derivatives selectively target mammalian DNA topoisomerase I (Top1) (Bjornsti et al., 1989; Hsiang et al., 1985; Marchand et al., 2006; Nitiss and Wang, 1988; Pommier et al., 2003), and are effective anticancer drugs (Adams et al., 2006; Capranico et al., 2004; Garcia-Carbonero and Supko, 2002; Pizzolato and Saltz, 2003; Wall and Wani, 1995). By trapping the DNA-Top1 intermediate these drugs form a ternary complex, which upon encountering a replication fork becomes a lethal lesion leading to drug-induced cytotoxicity (Pommier et al., 2003). As the camptothecins are not covalently linked to either the DNA or Top1, the drug-DNA-Top1 ternary complex is transient and rapidly reversible (Marchand et al., 2006; Staker et al., 2002). This reversibility/instability of the ternary complex necessitates prolonged drug treatment to achieve clinical anticancer activity. One way to circumvent this limitation is to develop drugs that increase the stability of the drug-DNA-Top1 ternary complex.

Following the discovery that NSC314622 was a Top1 inhibitor (Kohlhagen et al., 1998), several indenoisoquinolines have been shown to overcome some of the limitations posed by the camptothecins (Antony et al., 2003; Meng et al., 2003) (Fig. 1). Crystallography experiments show that the indenoisoquinolines, like the camptothecins, trap the DNA-Top1 intermediate by forming a network of hydrogen bonds with Top1 amino acid residues and by  $\pi$ -stacking interactions between the intercalated molecule and the DNA base pairs flanking the Top1 cleavage site without being covalently linked (Ioanoviciu et al., 2005; Marchand

et al., 2006; Staker et al., 2005) (Fig. 2B). To increase the affinity of the indenoisoquinolines for DNA and to reduce their dissociation from the Top1 cleavage complexes, we have synthesized several bisindenoisoquinolines, which differ by their linker lengths and symmetry (*Nagarajan, Morrell, Antony, Kohlhagen, Agama, Pommier, Hollingshead and Cushman, submitted*). While the bisindenoisoquinoline-DNA-Top1 ternary complexes are still reversible, we reasoned that the advantage conferred by the bisindenoisoquinolines would be that one of the two indenoisoquinoline rings could intercalate inside the cleavage site of the Top1 cleavage complex while the other could bind immediately downstream, and thereby stabilize the DNA-Top1- drug complex (Fig. 2C & D).

Bifunctional intercalators were developed as anticancer drugs as early as the 1970's with the diacridines (Canellakis et al., 1976; Le Pecq et al., 1975) and 1980's with 7H-pyridocarbazole dimers (Garbay-Jaureguiberry et al., 1987; Markovits et al., 1986; Pelaprat et al., 1980). More recent are bisintercalators from amonafide, elinafide, imidazonaphthalimides, 9-aminoacridine and anthracyclines (Brana et al., 2004; Nair et al., 2005). Targeting of Top1 with bisintercalators is further supported by inhibition of topoisomerase II (Top2) with acridine conjugates (Wang et al., 2001). The parent polyamines, spermine and spermidine, have limited activity on Top2 (Fesen and Pommier, 1989) but the bis-substituted spermine derivatives are efficient Top2 inhibitors compared to their monosubstituted spermidine counterparts (Wang et al., 2001).

This current study focuses on the bisindenoisoquinoline NSC 727357 (for structure see Fig. 1). Although initial biochemical testing with purified Top1

showed limited activity, NSC 727357 was studied further because it was found active in the animal hollowfiber assay. Here we show that NSC 727357 having two indenoisoquinoline pharmacophores not only exhibits site-specific Top1 inhibition but also acts as a DNA intercalator and as a Top2 inhibitor. The bisindenoisoquinoline NSC 727357 exhibits cytotoxicity against a wide range of cancer cell lines that is only partially Top1- and p53-dependent. The promising hollow fiber score and activity against melanoma xenografts make the bisindenoisoquinoline NSC 727357 a novel anticancer drug candidate.

## MATERIALS AND METHODS

**Drugs, Enzymes, and Chemicals.** Camptothecin (CPT) was obtained from the Drug Synthesis and Chemistry Branch, National Cancer Institute (Bethesda, MD). The syntheses of NSC 314622 (Cushman and Cheng, 1978), MJ-III-65 (NSC 706744) (Cushman et al., 2000), and the monomer NSC 725671 (Nagarajan et al., 2004) have been previously described. The synthesis of the bisindenoisoquinoline NSC 727357 will be described elsewhere (*Nagarajan, Morrell, Antony, Kohlhagen, Agama, Pommier, Hollingshead and Cushman, submitted*). Etoposide (VP-16) was purchased from Sigma (St. Louis, MO). Drug stock solutions were made in DMSO at 100 mM for VP-16 and 5 mM for CPT and the indenoisoquinolines. Aliquots were stored at  $-20^{\circ}\text{C}$  and further dilutions were made in DMSO immediately before use. The final concentration of DMSO in the reaction mixtures did not exceed 10% (v/v).

Recombinant human Top1 (Top1) was purchased from TopoGen Inc. (Port Orange, FL). T4 polynucleotide kinase, DNA polymerase I (Klenow fragment), dNTP [where N is A (adenosine), C (cytosine), G (guanosine) or T (thymine)],  $\phi\text{X174}$  DNA, agarose and polyacrylamide/bis were purchased from Invitrogen (Carlsbad, CA) or New England Biolabs (Beverly, MA). DNA quick spin columns were purchased from Roche Diagnostics Corporation (Indianapolis, IN).  $[\gamma^{32}\text{P}]$ -deoxyATP and  $[\alpha^{32}\text{P}]$ -deoxyGTP 5'-triphosphate were purchased from DuPont-New England Nuclear (Boston, MA). Oligonucleotides were synthesized by MWG-Biotech (High Point, NC).

**Top1 reactions.** The 161-bp fragment from pBluescript SK (-) phagemid DNA (Stratagene, La Jolla, CA) was 3'-end-labeled with [ $\alpha^{32}\text{P}$ ]-dGTP as described previously (Antony et al., 2003). For Top1 cleavage assays, labeled DNA (~50 fmole/reaction) was incubated with 5 ng recombinant Top1 with or without drug at 25°C in 10  $\mu\text{l}$  reaction buffer (10 mM Tris-Cl pH 7.5, 50 mM KCl, 5 mM  $\text{MgCl}_2$ , 0.1 mM EDTA, 15  $\mu\text{g/ml}$  BSA, final concentrations).

To the reaction mixtures, 3.3 volumes of Maxam Gilbert loading buffer (80% formamide, 10 mM sodium hydroxide, 1 mM sodium EDTA, 0.1% xylene cyanol, and 0.1% bromophenol blue, pH 8.0) were added. Aliquots were separated in 16% denaturing polyacrylamide gels (7M urea) in 1X TBE (45 mM Tris, 45 mM Boric acid, 1 mM EDTA) for 2 h at 40 V/cm at 50°C.

Imaging and quantitation were performed using a Phosphorimager (Molecular Dynamics, Sunnyvale, CA).

**Top2-Mediated DNA Cleavage Assays.** The same pSK fragment used for Top1 assays or single-stranded oligonucleotides were 5'-end-labeled with [ $\gamma^{32}\text{P}$ ]-ATP and T4 polynucleotide kinase (Khan et al., 2003). Labeling mixtures were subsequently centrifuged through mini quick spin DNA columns (for pSK fragment) or Oligo columns (for oligonucleotides) (Roche Diagnostics Corporation, Indianapolis, IN) to remove the unincorporated label. Annealing to the complementary strand of the oligonucleotides was performed by heating the reaction mixture to 95°C and overnight cooling to room temperature in 10 mM



Tris·HCl (pH 7.8), 100 mM NaCl, 1 mM EDTA.

DNA substrates (~10 pmol per reaction) were incubated with 500 ng of Top2 in the presence or absence of drugs for the indicated times at 25°C in 10  $\mu$ l reaction buffer (10 mM Tris·HCl, pH 7.5, 50 mM KCl, 5 mM MgCl<sub>2</sub>, 1 mM ATP, 0.2 mM DTT, 0.1 mM EDTA, 15  $\mu$ g/ml BSA) (Khan et al., 2003). Reactions were stopped by adding SDS (final concentration 0.5%). Samples were separated on 16% (for pSK DNA) or 20% (for the oligonucleotides) denaturing polyacrylamide gels (7 M urea). Imaging and quantitation were performed using a Phosphorimager (Molecular Dynamics, Sunnyvale, CA).

**$\phi$ X174 DNA unwinding assay.** Reaction mixtures (10  $\mu$ l final volume) contained 0.3  $\mu$ g supercoiled  $\phi$ X174 DNA in reaction buffer (10 mM Tris·HCl, pH 7.5, 50 mM KCl, 5 mM MgCl<sub>2</sub>, 0.1 mM EDTA, and 15  $\mu$ g/ml bovine serum albumin) and 2 units of Top1 (Pommier et al., 1987). Reactions were performed at 37°C for 30 min with Top1 alone followed by incubation in the presence or absence of drug for another 30 min. The reactions were terminated by the addition of 0.5% SDS and 0.5 mg/ml proteinase K. Samples were incubated for 30 min at 50°C. Next, 1.2  $\mu$ l of 10X loading buffer (20% Ficol 400; 0.1 M Na<sub>2</sub>EDTA, pH 8.0, 1.0% SDS, and 0.25% bromphenol blue) were added and reactions mixtures were loaded onto a 1% agarose gel made in 1X TBE buffer. Gels were run in 1X TBE containing 0.1% SDS. After electrophoresis, DNA bands were stained in 10  $\mu$ g/ml of ethidium bromide and visualized by transillumination with ultraviolet light (300 nm).

**Flow cytometry analysis of DNA content.** Cell cycle analyses were done with a FACScan flow cytometer (Becton Dickinson, Sunnyvale, CA). Cell cycle distributions were calculated using ModFit *LT* software (Verity Software House, Inc., Topsham, ME).

**Two-dimensional flow cytometry analysis: DNA content and BrdU incorporation.** Cells were pulse-labeled with 50  $\mu\text{mol/L}$  BrdU during the last 30 minutes of treatment. Cells were collected, fixed in 70% ethanol at 4°C, washed with PBS and resuspended in 3 ml of 2N HCl and incubated at room temperature for 30 min. To each tube 6 ml of 0.1 M sodium borate (pH 8.5) were added to neutralize the pH. Cells were spun down and washed twice with PBS containing 0.5% Tween-20 and 0.5% BSA. Cells were pelleted by centrifugation and resuspended in 20  $\mu\text{L}$  of FITC-conjugated anti-BrdU antibody (Becton Dickinson, Franklin Lakes, NJ). After incubation with the anti-BrdU antibody in the dark at room temperature for 1 h, the pellets were washed twice with PBS-Tween-BSA and resuspended in 500  $\mu\text{L}$  of propidium iodide (PI) solution (50  $\mu\text{g/ml}$  PI and 50  $\mu\text{g/ml}$  RNase). Analyses were done with a FACScan flow cytometer.

**Cell lines and cytotoxicity assays.** P388 and P388 Top1-deficient murine leukemia cells were a kind gift from Michael R. Mattern and Randal K. Johnson (GlaxoSmithKline, King of Prussia, PA) and maintained in RPMI 1640 medium (Invitrogen) containing 10% fetal bovine serum (FBS) (Atlanta

Biologicals, Norcross, GA). The P388 Top1-deficient cells were obtained by exposing CPT-5 cells to stepwise increasing concentrations of CPT until they grew in the presence of 45  $\mu$ M CPT (Mattern et al., 1991). Human colon HCT-116 and breast cancer MCF-7 cells were purchased from American Type Culture Collection (Manassas, VA). The HCT-116 Top1-siRNA (HCT-116-siTop1) and MCF-7 Top1-siRNA (MCF-7-siTop1) cells were derived as described (Sordet et al., 2004) (Miao & Pommier, unpublished data). HCT-116 and MCF-7 cells were maintained in DMEM supplemented with 10% FBS. All cells were maintained in a 5% CO<sub>2</sub> incubator at 37°C. TK6 and NH32 are EBV-immortalized human lymphoblastoid cell lines (gift of Dr. Howard Liber, Colorado State University, Fort Collins, CO) and were maintained at 5-10 x 10<sup>5</sup> cells/ml in RPMI-1640 medium, supplemented with 10% FBS, glutamine (0.3  $\mu$ g/ml), 100  $\mu$ g/ml streptomycin sulfate and 100 U/ml penicillin G. TK6 has wild-type p53 and NH32 is an isogenic cell line generated by p53-targeted deletion and expresses no p53 protein. Both these cell lines have comparable growth kinetics.

Cytotoxicity of the bisindenoisoquinoline NSC 727357 and MJ-III-65 (NSC 706744) in wild-type P388 and P388 Top1-deficient cells was assessed by MTT (Sigma-Aldrich) colorimetric assay as described (Antony et al., 2005). Their cytotoxicity in human colon cancer HCT-116 or HCT-116-siTop1 cells or human breast cancer MCF-7 or MCF-7-siTop1 cells was assessed by the sulforhodamine B (SRB) (Sigma-Aldrich Co., St. Louis, MO) assay. Growth kinetics of the wild-type cell line and its corresponding Top1-deficient or siTop1 cells was comparable. Drug treatment was continuous for 3 days for both the

MTT and SRB assays. Determinations for all experiments were made in duplicates, and the results were expressed as mean  $\pm$  S.D. Percentage of growth was calculated relative to control (vehicle treated cells) after 3 days of culture with control taken as 100.

For growth inhibition assay of non-adherent TK6 and NH32 cell lines, the cells were seeded at 20,000 cells/well in sixtuplicates in 96-well plates and the drugs were added in serial dilutions in the medium. Dose-response curves were generated using the Cell Titer 96 Aqueous One Solution Cell Proliferation Assay (Promega, Madison, WI), a colorimetric method for determining the number of viable cells based on bio-reduction of a tetrazolium compound (MTS) by metabolically active cells. After 24 h of exposure to a single drug, 20  $\mu$ l of MTS reagent were added to each well and the plates were incubated in a humidified 37°C incubator with 5% CO<sub>2</sub> for 1-4 h. Absorbance at 490 nm was recorded using a 96-well plate reader. For consistency across experiments and to ensure a linear response between cell number and absorbance, the background-corrected target absorbance value for untreated cells was kept at 0.9-1.0 in all plates. Data was averaged and normalized against the non-treated controls to generate dose-response curves.

**Hollow fiber assays.** The bisindenoisoquinoline NSC 727357 was evaluated in the hollow fiber assay as a preliminary *in vivo* experiment to provide qualitative indications of drug efficacy. In the hollow fiber model, polyvinylidene fluoride fibers containing various human cancer cell cultures (12 tumor cell lines)

were implanted intraperitoneally (ip) and subcutaneously (sc) into athymic nude mice and NSC 727357 was administered by the ip route at two dose levels. The effect of the drug was assessed by comparing the viable cancer cell mass in hollow fibers from drug-treated mice to those of fibers from vehicle-treated control mice. To simplify evaluation, the protocol adopts a point system that allows rapid viewing of the activity of a given compound. For this, a value of 2 is assigned for each drug dose that results in a 50% or greater reduction in viable cell mass compared to controls. The maximum possible score for an agent is 96 (12 cell lines × 2 sites × 2 dose levels × 2 [score]). Compounds with a combined ip + sc score of 20, an sc score of 8, or a net cell kill of one or more cell lines are considered indicative of potential activity (Decker et al., 2004).

**Activity against human tumor xenografts.** The *in vivo* efficacy of the bisindenoisoquinoline NSC 727357 was evaluated in the human melanoma xenograft LOX IMVI. Briefly, the tumor was maintained by serial *in vivo* passage in athymic nude mice (nu/nuNCr). For the drug study, tumors implanted in the axillary region were allowed to reach approximately 88 mg prior to the start of treatment. The tumor weight was calculated from the length and width measurements obtained from caliper measurements. The formula used was tumor weight (in mg) = [(tumor length × tumor width<sup>2</sup>)/2]. NSC 727357 was formulated as a solution in 10% DMSO in saline containing 0.05% Tween-80 and administered by the ip route. A group of 20 mice served as vehicle controls. A single maximum tolerated dose (MTD) was determined prior to selection of the

experimental doses. The single intraperitoneal dose MTD was determined to be 100 mg/kg. Using this MTD, treatment doses were determined using the formula:  $\text{dose} = [(1.5 \times \text{MTD})/\text{number of doses given}] = [(1.5 \times 100)/5] = 30 \text{ mg/kg/dose}$ . The lower doses were selected based upon a 0.67 stepdown, i.e.,  $30 \text{ mg/kg} \times 0.67 = 20 \text{ mg/kg} \times 0.67 = 13.4 \text{ mg/kg}$ . While this does not represent a formal determination of the MTD for the particular route, schedule and vehicle selected, it is the mechanism by which the preliminary test doses for newly evaluated compounds are selected by the DTP, as their response represent a reasonable starting point. Doses of 13.4, 20 and 30 mg/kg/dose were administered once daily for 5 days, with the first treatment given on day 7 post tumor implantation (QD  $\times$  5, day 7). The number of animals per group were:  $n = 18$  for the vehicle treated group and  $n = 9$  for each of the drug treated groups. Percent growth inhibition in the drug-treated tumors was compared to the vehicle-control treated animals.

## RESULTS

**The bisindenoisoquinoline NSC 727357 induces Top1-mediated DNA cleavage complexes.** Because indenoisoquinolines are known Top1 inhibitors (Antony et al., 2003; Kohlhagen et al., 1998; Meng et al., 2003), the activity of NSC 727357 was examined in the presence of purified Top1. As shown in Figure 3A, NSC 727357 traps Top1 cleavage complexes at submicromolar drug concentrations. Cleavage of DNA by Top1 alone can be visualized depending on the activity of the Top1 enzyme preparation (as seen in Fig. 3A lane 2). The overall pattern of cleavage sites trapped by NSC 727357 is different from CPT or from the indenoisoquinoline MJ-III-65 (NSC 706744) (Antony et al., 2003). Among the three main cleavage sites induced by the bisindenoisoquinoline NSC 727357, two are common to CPT (sites 70 and 92) and the other to MJ-III-65 (NSC 706744) (site 44). The Top1-mediated cleavage increases with the concentration of NSC 727357 from 0.1 to 1  $\mu\text{M}$ . However, cleavage was suppressed at higher concentrations (10 and 100  $\mu\text{M}$ ). For instance, cleavage at site 92 is reduced to below the level of cleavage seen with Top1 alone (Figs. 3A & 3C). This inhibition of Top1 catalytic activity at higher concentrations (10 and 100  $\mu\text{M}$ ) of NSC 727357 could be due to DNA intercalation outside the Top1 cleavage complexes (as shown in Fig. 2E). Assessing the stability of the DNA-Top1 cleavage by reversal experiments have been attempted. However, reliable data could not be generated as the Top1-mediated DNA cleavage induced by

NSC 727357 is relatively low [approximately 2-fold over that of Top1 alone (Fig. 3C)].

In comparison, the monomer NSC 725671, while trapping Top1 cleavage complexes at similar sites, has a lower affinity for site 70. Moreover, higher concentrations (10-100  $\mu\text{M}$ ) of the monomer are required to achieve levels of cleavage comparable to the bisindenoisoquinoline (see Fig. 3B). Hence, the bisindenoisoquinoline NSC 727357 traps Top1-cleavage complexes more efficiently than its corresponding monomer.

**DNA unwinding and inhibition of Top1 catalytic activity by the bisindenoisoquinoline NSC 727357.** To further elucidate the DNA intercalating effect of NSC 727357, DNA unwinding studies were carried out in the presence of excess Top1 (Pommier et al., 1987). As seen in Figure 4A, the DNA relaxed by Top1 alone (lane 2) generates a family of DNA topoisomers with slow electrophoretic mobility. The drug was then added while Top1 was kept in the reaction mixture. Upon increasing the concentration of NSC 727357, the DNA was progressively supercoiled, indicating that NSC 727357 intercalates into DNA (Pommier et al., 1987).

An interesting feature observed at high concentrations of NSC 727357 (30 and 100  $\mu\text{M}$ , lanes 8 and 9 respectively) is that, along with fully supercoiled DNA is the persistence of relaxed DNA. Since we start with relaxed DNA isomers before the addition of the drug (lane 2), the inability of Top1 to completely process the DNA at higher drug concentrations (30 and 100  $\mu\text{M}$ ; lanes 8 & 9) as



compared to lower concentrations (10  $\mu$ M; lane 7), indicates the partial inhibition of Top1 DNA-cleaving activity by NSC 727357. This inhibition of Top1 relaxation activity is consistent with the Top1 cleavage data (Fig. 3B & 3C) where NSC 727357 inhibited Top1-mediated DNA cleavage at high drug concentrations ( $\geq 10$   $\mu$ M). In other words, NSC 727357 acts as a Top1 poison at low concentrations (<10  $\mu$ M) and a Top1 suppressor at high concentrations (>10  $\mu$ M).

The monomer (NSC 725671) like the bisindenoisoquinoline (NSC 727357) also supercoils DNA but requires higher concentrations to achieve the same effect (compare lanes 3-4 and 8-9 of Fig. 4B). This reduced activity of the monomer is consistent with what was previously observed for the trapping of Top1 cleavage complexes by the monomer (Fig. 3B). From the above data, we conclude that the bisindenoisoquinoline NSC 727357 traps Top1-DNA cleavage complexes at low concentrations (<10  $\mu$ M) and inhibits Top1 catalytic activity at higher drug concentrations (>10  $\mu$ M) as it supercoils the DNA by intercalation.

**The bisindenoisoquinoline NSC 727357 also traps Top2 cleavage complexes.** Because DNA intercalators are known to trap Top2 (Tewey et al., 1984) we tested whether NSC 727357 also targets Top2. Cleavage assays were carried out using the same DNA fragment used previously for the Top1 experiments. Figure 5A shows that at low concentrations (<10  $\mu$ M), the bisindenoisoquinoline NSC 727357 traps Top2-DNA cleavage complexes at a single site (dashed arrow) in the DNA fragment analyzed. To determine the DNA sequence at this site of cleavage, a duplex oligonucleotide (sequence shown in

Fig. 5D) was designed spanning the region of the cleavage site. Figure 5B shows that the bisindenoisoquinoline NSC 727357 traps Top2 at a “concerted” site on both the upper and lower strands (Bromberg et al., 2004; Khan et al., 2003). This site is also trapped by the known Top2 inhibitor etoposide (VP-16). The extent of cleavage observed increases with concentrations up to 0.1  $\mu$ M NSC 727357 (Figs. 5B & 5C) with greater cleavage observed on the lower strand (Figs. 5B & 5D, solid arrow). We conclude that NSC 727357 is able to trap both Top1- and Top2- cleavage complexes at submicromolar drug concentrations.

**The bisindenoisoquinoline NSC 727357 leads to cell cycle arrest in G1 without significant inhibition of thymidine incorporation.** To evaluate the effect of NSC 727357 on cell cycle progression, human colon carcinoma HT29 cells were treated with varying doses of NSC 727357 for 18 h. Drug-treated cells accumulated in the G1-phase of the cell cycle (Fig. 6B). With increasing drug concentration the cells became apoptotic (not shown). This profile is very different from that observed with known Top1 inhibitors like CPT or the indenoisoquinoline MJ-III-65 (NSC 706744), which induce dose-dependent accumulation of cells in the S- and G2-phases of the cell cycle (Fig. 6C) (Antony et al., 2003; Shao et al., 1997).

S-phase accumulation with known Top1 inhibitors is associated with inhibition of DNA synthesis (Shao et al., 1999). To assess the effect of NSC 727357 on DNA synthesis, BrdU incorporation experiments were carried out. As expected, CPT inhibited BrdU incorporation in cells predominantly in late S-

phase (Fig 7B). The bisindenoisoquinoline NSC 727357 did not show any significant inhibition of BrdU incorporation when cells were treated for 1 hr with 1 or 5  $\mu$ M. This clearly indicates that while NSC 727357 is an inhibitor of topoisomerases, its cellular effects are different from known Top1 and Top2 inhibitors.

**NSC 727357 kills cells independently of Top1.** To assess the role Top1 plays in the cytotoxicity of the bisindenoisoquinoline NSC 727357, Top1-deficient and Top1-siRNA cells were used. As observed in Figure 8A, Top1-deficient P388 cells (Antony et al., 2005) and MCF-7-siTop1 cells (Miao & Pommier, unpublished) showed partial resistance to NSC 727357 at low drug concentrations ( $<1$   $\mu$ M). However, this was not observed in HCT-116-siTop1 cells. In contrast, resistance to MJ-III-65 (NSC 706744), was observed in all three cell pairs with Top1 deficiency or silencing (Fig. 8B). These results demonstrate that additional targets mediate NSC 727357-mediated cell killing independently from Top1.

**NSC 727357 kills cells independently of p53.** Consistent with previously published results (Bozko et al., 2002; Li et al., 2000), CPT-induced cell killing is largely p53-dependent. Loss of cell viability measured by cytotoxicity assay at 24 h of exposure to CPT showed an  $IC_{50} \approx 5$  nM for cells with wild-type p53 (TK6), whereas an  $IC_{50} \approx 300$  nM was observed for p53-null NH32 cells (Fig. 9A). Similar to CPT, dependence on p53 was observed for NSC 706744. The  $IC_{50}$  for

NSC 706744 was 25 nM for p53 wild-type TK6 versus 1250 nM for p53-null NH32 (Fig. 9B). By contrast, NSC 727357 showed only a 3-fold difference between the p53-wild-type and p53-null cells (IC<sub>50</sub> of 300 nM for TK6 and 1  $\mu$ M for NH32; Fig. 9C).

**Cytotoxicity profile of NSC 727357 in the NCI60.** Fig. 10 shows the cytotoxicity profile of NSC 727357 as a mean graph representation and the comparison between the cytotoxicity profiles of NSC 727357, NSC 706744 and CPT. The mean GI<sub>50</sub> across the cell lines (MG\_MID) are 0.067  $\mu$ M for NSC 727357, 0.1  $\mu$ M for NSC 706744 and 0.044  $\mu$ M for CPT respectively. The activity pattern of NSC 727357 across the 60 cell lines is different from those of NSC 706744 and CPT, which are comparable to each other. Accordingly, the COMPARE analysis for NSC 727357 showed no correlation with NSC 706744 and CPT.

**Antitumor activity of the bisindenoisoquinoline NSC 727357 in hollow fiber assay and melanoma xenografts.** The data in Figure 11A summarize the hollow fiber activity of NSC 727357 administered by intraperitoneal injection at two dose levels (30 and 20 mg/kg/dose) on a once daily for four days (QD X 4) schedule. After treatment, the collected fibers were subjected to a stable-endpoint MTT assay. A 50% or greater reduction in percent net growth in the treated samples compared to the vehicle control samples was given a score of 2 for each of the 12 cell lines evaluated. The individual intraperitoneal and subcutaneous scores of the two doses 20 and 30 mg/kg combined are represented in Figure 11A. A compound is referred for xenograft testing if the

combined ip + sc score is 20 or greater. Compared to the most effective standard Taxol (total score 38), the bisindenoisoquinoline NSC 727357 showed a similar subcutaneous score (=6). Moreover, NSC 727357 showed a high total score of 32 (out of 96 possible). Because of its activity in the Hollow fiber assay, NSC 727357 was tested in a xenograft model.

Figure 11B shows the antitumor activity of NSC 727357 (13.4, 20 and 30 mg/kg/dose) administered i.p. QD X 5, day 7 in female athymic nude mice (nu/nuNCr) bearing early stage subcutaneous LOX-IMVI melanoma xenografts. The compound was assessed in a preliminary study against LOX-IMVI because it was one of the tumor cell lines that demonstrated growth inhibition in the hollow fiber assay. The bisindenoisoquinoline NSC 727357 was active against the melanoma xenografts with a reduction in median tumor weight on day 14 of 24% in the 13.4 mg/kg group, 33% in the 20 mg/kg group and 56% in the 30 mg/kg drug-treated group. The high test dose (30 mg/kg) was associated with a 22% body weight loss and 2/9 animals dying of presumed compound-related toxicity. In the mid and low dose groups there was average percent body weight losses of 19.7% and 12.2% respectively. The vehicle control treated mice did not lose body weight during the experiment. Our results with the LOX-IMVI xenografts is not intended to suggest that it is the most sensitive or responsive xenograft. Moreover, additional dosing schedule may reveal optimal activity. While pharmacology and efficacy optimization studies have yet to be standardized for NSC 727357, our preliminary animal data indicates that NSC 727357 impacts a rapidly growing tumor under suboptimal conditions. Based on the good hollow

fiber score and preliminary evidence of *in vivo* antitumor activity, NSC 727357 appears worthy of consideration for preclinical development.

## DISCUSSION

Our efforts are focused on developing novel Top1 inhibitors that would overcome the limitations imposed by camptothecins. To date, we have synthesized a large series of indenoisoquinolines that are chemically stable, exhibit unique cleavage preferences and form Top1-DNA cleavage complexes that reverse more slowly than those formed by camptothecin (CPT) (Antony et al., 2005; Ioanoviciu et al., 2005; Morrell et al., 2004; Nagarajan et al., 2004; Nagarajan et al., 2003; Strumberg et al., 1999; Xiao et al., 2004; Xiao et al., 2005). In this study we explored the possibility of using bisindenoisoquinolines, which, because of their ability to intercalate DNA could form stable Top1-DNA-drug complexes, making them potent Top1 inhibitors compared to their corresponding monomers (see Fig. 2).

Initial cytotoxicity screening in the NCI-60 cell line panel with the bisindenoisoquinoline NSC 727357 revealed this compound to be a good drug candidate with an MGM value of 0.067  $\mu\text{M}$  (Fig. 10). This antiproliferative activity was further supported by *in vivo* studies in hollow fiber assays (score of 32) and in melanoma xenografts treated with 30 mg/kg NSC 727357 (53% reduction in median tumor weight) (see Fig 11). Because of its antitumor activity, the bisindenoisoquinoline NSC 727357 was further investigated to evaluate its molecular and cellular pharmacological target(s).

Structurally, the bisindenoisoquinoline NSC 727357 contains two aromatic nuclei that are linked by a polyaminoalkyl spacer (as shown in Fig. 1). The design of bisindenoisoquinoline NSC 727357 was based on recent crystallographic

analysis of the orientation of indenoisoquinolines within the Top1-DNA-drug ternary complex (Ioanoviciu et al., 2005; Marchand et al., 2006; Staker et al., 2005). From the crystal structures it is apparent that the long axis of the aromatic indenoisoquinoline nucleus lies parallel to the long axis of the DNA base pairs (Ioanoviciu et al., 2005; Marchand et al., 2006; Staker et al., 2005) (see Fig. 2B). Accordingly, we hypothesize that one of the bisindenoisoquinoline chromophores would be intercalated between the base pairs immediately flanking the cleavage site (by convention positions -1 and +1) (see Fig. 2C). Intercalation was confirmed by DNA unwinding assays (Pommier et al., 1987) (see Fig. 4). When tested against Top1, the bisindenoisoquinoline NSC 727357 as compared to its monomer was a potent Top1 inhibitor at low drug concentrations (0.1 and 1  $\mu\text{M}$ ) and a catalytic inhibitor of Top1 at higher drug concentrations ( $\geq 10$   $\mu\text{M}$ , see Figs. 3 & 4). This is noteworthy, as the bisindenoisoquinoline NSC 727357 with its size is probably the bulkiest known Top1 inhibitor. Inhibition of Top1 cleavage complexes at higher concentrations (10 and 100  $\mu\text{M}$ , see Fig. 3A) is probably due to additional intercalation upstream from the Top1 cleavage site (Fig. 2E). Indeed, experiments with a single polycyclic benzo[a]pyrene dA adduct showed that intercalation upstream from the Top1 cleavage site blocks Top1-mediated DNA cleavage (Pommier et al., 2000). Additionally, the bisindenoisoquinoline NSC 727357 was able to trap Top2 (Fig. 5). Thus, the bisindenoisoquinoline NSC 727357 appears to be very much like actinomycin D and morpholinodoxorubicin that are dual Top1 and Top2 inhibitors as well as DNA intercalators (Wassermann et al., 1990). Top1 and Top2 inhibition at high drug



concentration ( $\geq 10 \mu\text{M}$ ) is probably due to the intercalation at inhibitory sites (Pommier et al., 2000) or to multiple drugs bound at the Top1 site (see Fig. 2E).

While it is evident that the bisindenoisoquinoline NSC 727357 does inhibit Top1 *in vitro*, the dependence on Top1 for exerting its cytotoxicity is partial (Fig. 8A). Also in treated cells, at drug concentrations that are antiproliferative, we have been unable to detect NSC 7272357-induced Top1-DNA complexes (data not shown). Hence, NSC 727357 is clearly different from other known Top1 inhibitors like CPT or the indenoisoquinoline NSC 706744 (Fig. 8B) where Top1 is the primary cellular target. Moreover, cells treated with the bisindenoisoquinoline NSC 727357 tended to arrest at the G1 phase of the cell cycle as compared to NSC 706744 (Fig. 6) or CPT that cause an early G2/M block followed by an S-phase arrest (Goldwasser et al., 1996; Jones et al., 2000; Shao et al., 1997). Absence of an S-phase arrest was further supported by lack of significant inhibition of DNA synthesis on treatment with NSC 727357 (Fig. 7). Also striking was the minimal dependence on p53 for the antiproliferative activity of the bisindenoisoquinoline NSC 727357 (Fig. 9). Studies are underway to explore the significance of the G1 phase arrest induced by NSC 727357 irrespective of Top1 and p53 status.

The apparent lack of Top1- or p53-dependence for the antiproliferative activity of NSC 727357, along with an absence of S-phase arrest and inhibition of DNA synthesis on drug treatment implies that the bisindenoisoquinoline NSC 727357 has additional targets besides Top1 or Top2. The ability to intercalate DNA could account for these unique features. The unique activity profile of NSC

727357 is further supported by the COMPARE analysis performed in the NCI's database using the GI50 values. Using NSC 727357 as a seed in the COMPARE analysis, we found only 6 compounds that were identified with Pearson correlation coefficients greater than 0.5. Of the six, five compounds were members of the anthracycline family of natural products that interact with DNA, either as intercalating agents, minor groove binders or inhibitors of Top2. Other biological targets besides Top1 are clearly involved in the activities of the bisindenoisoquinolines. Though the bisindenoisoquinoline NSC 727357 differs from other indenoisoquinoline Top1 inhibitors, its good antiproliferative and antitumor activity make it a candidate for consideration for therapeutic development.

## REFERENCES

- Adams DJ, da Silva MW, Flowers JL, Kohlhagen G, Pommier Y, Colvin OM, Manikumar G and Wani MC (2006) Camptothecin analogs with enhanced activity against human breast cancer cells. I. Correlation of potency with lipophilicity and persistence in the cleavage complex. *Cancer Chemother Pharmacol* **57**(2):135-144.
- Antony S, Jayaraman M, Laco G, Kohlhagen G, Kohn KW, Cushman M and Pommier Y (2003) Differential induction of topoisomerase I-DNA cleavage complexes by the indenoisoquinoline MJ-III-65 (NSC 706744) and camptothecin: base sequence analysis and activity against camptothecin-resistant topoisomerases I. *Cancer Res* **63**(21):7428-7435.
- Antony S, Kohlhagen G, Agama K, Jayaraman M, Cao S, Durrani FA, Rustum YM, Cushman M and Pommier Y (2005) Cellular topoisomerase I inhibition and antiproliferative activity by MJ-III-65 (NSC 706744), an indenoisoquinoline topoisomerase I poison. *Mol Pharmacol* **67**(2):523-530.
- Bjornsti MA, Benedetti P, Viglianti GA and Wang JC (1989) Expression of human DNA topoisomerase I in yeast cells lacking yeast DNA topoisomerase I: restoration of sensitivity of the cells to the antitumor drug camptothecin. *Cancer Res* **49**(22):6318-6323.
- Bozko P, Larsen AK, Raymond E and Skladanowski A (2002) Influence of G2 arrest on the cytotoxicity of DNA topoisomerase inhibitors toward human carcinoma cells with different p53 status. *Acta Biochim Pol* **49**(1):109-119.

- Brana MF, Cacho M, Garcia MA, de Pascual-Teresa B, Ramos A, Dominguez MT, Pozuelo JM, Abradelo C, Rey-Stolle MF, Yuste M, Banez-Coronel M and Lacal JC (2004) New analogues of amonafide and elinafide, containing aromatic heterocycles: synthesis, antitumor activity, molecular modeling, and DNA binding properties. *J Med Chem* **47**(6):1391-1399.
- Bromberg KD, Velez-Cruz R, Burgin AB and Osheroff N (2004) DNA ligation catalyzed by human topoisomerase II alpha. *Biochemistry* **43**(42):13416-13423.
- Canellakis ES, Fico RM, Sarris AH and Shaw YH (1976) Diacridines - double intercalators as chemotherapeutic agents. *Biochem Pharmacol* **25**(2):231-236.
- Capranico G, Zagotto G and Palumbo M (2004) Development of DNA topoisomerase-related therapeutics: a short perspective of new challenges. *Curr Med Chem Anticancer Agents* **4**(4):335-345.
- Cushman M and Cheng L (1978) A stereoselective oxidation by thionyl chloride leading to the indeno[1,2-c] isoquinoline system. *J Org Chem* **43**:3781.
- Cushman M, Jayaraman M, Vroman JA, Fukunaga AK, Fox BM, Kohlhagen G, Strumberg D and Pommier Y (2000) Synthesis of new indeno[1,2-c]isoquinolines: cytotoxic non-camptothecin topoisomerase I inhibitors. *J Med Chem* **43**(20):3688-3698.
- Decker S, Hollingshead M, Bonomi CA, Carter JP and Sausville EA (2004) The hollow fibre model in cancer drug screening: the NCI experience. *Eur J Cancer* **40**(6):821-826.

Fesen M and Pommier Y (1989) Mammalian topoisomerase II activity is modulated by the DNA minor groove binder distamycin in simian virus 40 DNA. *J Biol Chem* **264**(19):11354-11359.

Garbay-Jaureguiberry C, Esnault C, Delepierre M, Laugaa P, Laalami S, Le Pecq JB and Roques BP (1987) Rational design of bis-intercalating drugs as antitumour agents: importance of rigidity in the linking chain. *Drugs Exp Clin Res* **13**(6):353-357.

Garcia-Carbonero R and Supko JG (2002) Current perspectives on the clinical experience, pharmacology, and continued development of the camptothecins. *Clin Cancer Res* **8**(3):641-661.

Goldwasser F, Shimizu T, Jackman J, Hoki Y, O'Connor PM, Kohn KW and Pommier Y (1996) Correlations between S and G2 arrest and the cytotoxicity of camptothecin in human colon carcinoma cells. *Cancer Res* **56**(19):4430-4437.

Hsiang YH, Hertzberg R, Hecht S and Liu LF (1985) Camptothecin induces protein-linked DNA breaks via mammalian DNA topoisomerase I. *J Biol Chem* **260**(27):14873-14878.

Ioanoviciu A, Antony S, Pommier Y, Staker BL, Stewart L and Cushman M (2005) Synthesis and mechanism of action studies of a series of norindenoisoquinoline topoisomerase I poisons reveal an inhibitor with a flipped orientation in the ternary DNA-enzyme-inhibitor complex as determined by X-ray crystallographic analysis. *J Med Chem* **48**(15):4803-4814.

- Jones CB, Clements MK, Wasi S and Daoud SS (2000) Enhancement of camptothecin-induced cytotoxicity with UCN-01 in breast cancer cells: abrogation of S/G(2) arrest. *Cancer Chemother Pharmacol* **45**(3):252-258.
- Khan QA, Kohlhagen G, Marshall R, Austin CA, Kalena GP, Kroth H, Sayer JM, Jerina DM and Pommier Y (2003) Position-specific trapping of topoisomerase II by benzo[a]pyrene diol epoxide adducts: implications for interactions with intercalating anticancer agents. *Proc Natl Acad Sci U S A* **100**(21):12498-12503.
- Kohlhagen G, Paull KD, Cushman M, Nagafuji P and Pommier Y (1998) Protein-linked DNA strand breaks induced by NSC 314622, a novel noncamptothecin topoisomerase I poison. *Mol Pharmacol* **54**(1):50-58.
- Le Pecq JB, Le Bret M, Barbet J and Roques B (1975) DNA polyintercalating drugs: DNA binding of diacridine derivatives. *Proc Natl Acad Sci U S A* **72**(8):2915-2919.
- Li G, Bush JA and Ho VC (2000) p53-dependent apoptosis in melanoma cells after treatment with camptothecin. *J Invest Dermatol* **114**(3):514-519.
- Marchand C, Antony S, Kohn KW, Cushman M, Ioanoviciu A, Staker BL, Burgin AB, Stewart L and Pommier Y (2006) A novel norindenoisoquinoline structure reveals a common interfacial inhibitor paradigm for ternary trapping of the topoisomerase I-DNA covalent complex. *Mol Cancer Ther* **5**(2)(February):287-295.
- Markovits J, Pommier Y, Mattern MR, Esnault C, Roques BP, Le Pecq JB and Kohn KW (1986) Effects of the bifunctional antitumor intercalator

- ditercalinium on DNA in mouse leukemia L1210 cells and DNA topoisomerase II. *Cancer Res* **46**(11):5821-5826.
- Mattern MR, Hofmann GA, McCabe FL and Johnson RK (1991) Synergistic cell killing by ionizing radiation and topoisomerase I inhibitor topotecan (SK&F 104864). *Cancer Res* **51**(21):5813-5816.
- Meng LH, Liao ZY and Pommier Y (2003) Non-camptothecin DNA topoisomerase I inhibitors in cancer therapy. *Curr Top Med Chem* **3**(3):305-320.
- Morrell A, Antony S, Kohlhagen G, Pommier Y and Cushman M (2004) Synthesis of nitrated indenoisoquinolines as topoisomerase I inhibitors. *Bioorg Med Chem Lett* **14**(14):3659-3663.
- Nagarajan M, Morrell A, Fort BC, Meckley MR, Antony S, Kohlhagen G, Pommier Y and Cushman M (2004) Synthesis and anticancer activity of simplified indenoisoquinoline topoisomerase I inhibitors lacking substituents on the aromatic rings. *J Med Chem* **47**(23):5651-5661.
- Nagarajan M, Xiao X, Antony S, Kohlhagen G, Pommier Y and Cushman M (2003) Design, synthesis, and biological evaluation of indenoisoquinoline topoisomerase I inhibitors featuring polyamine side chains on the lactam nitrogen. *J Med Chem* **46**(26):5712-5724.
- Nair RR, Wang H, Jamaluddin MS, Fokt I, Priebe W and Boyd DD (2005) A bisanthracycline (WP631) represses uPAR gene expression and cell migration of RKO colon cancer cells by interfering with transcription factor

- binding to a chromatin-accessible -148/-124 promoter region. *Oncol Res* **15**(5):265-279.
- Nitiss J and Wang JC (1988) DNA topoisomerase-targeting antitumor drugs can be studied in yeast. *Proc Natl Acad Sci U S A* **85**(20):7501-7505.
- Pelaprat D, Delbarre A, Le Guen I, Roques BP and Le Pecq JB (1980) DNA intercalating compounds as potential antitumor agents. 2. Preparation and properties of 7H-pyridocarbazole dimers. *J Med Chem* **23**(12):1336-1343.
- Pizzolato JF and Saltz LB (2003) Irinotecan (Campto) in the treatment of pancreatic cancer. *Expert Rev Anticancer Ther* **3**(5):587-593.
- Pommier Y, Covey JM, Kerrigan D, Markovits J and Pham R (1987) DNA unwinding and inhibition of mouse leukemia L1210 DNA topoisomerase I by intercalators. *Nucleic Acids Res* **15**(16):6713-6731.
- Pommier Y, Laco GS, Kohlhagen G, Sayer JM, Kroth H and Jerina DM (2000) Position-specific trapping of topoisomerase I-DNA cleavage complexes by intercalated benzo[a]-pyrene diol epoxide adducts at the 6-amino group of adenine. *Proc Natl Acad Sci U S A* **97**(20):10739-10744.
- Pommier Y, Redon C, Rao VA, Seiler JA, Sordet O, Takemura H, Antony S, Meng L, Liao Z, Kohlhagen G, Zhang H and Kohn KW (2003) Repair of and checkpoint response to topoisomerase I-mediated DNA damage. *Mutat Res* **532**(1-2):173-203.
- Shao RG, Cao CX, Shimizu T, O'Connor PM, Kohn KW and Pommier Y (1997) Abrogation of an S-phase checkpoint and potentiation of camptothecin



- cytotoxicity by 7-hydroxystaurosporine (UCN-01) in human cancer cell lines, possibly influenced by p53 function. *Cancer Res* **57**(18):4029-4035.
- Shao RG, Cao CX, Zhang H, Kohn KW, Wold MS and Pommier Y (1999) Replication-mediated DNA damage by camptothecin induces phosphorylation of RPA by DNA-dependent protein kinase and dissociates RPA:DNA-PK complexes. *Embo J* **18**(5):1397-1406.
- Sordet O, Khan QA, Plo I, Pourquier P, Urasaki Y, Yoshida A, Antony S, Kohlhagen G, Solary E, Saparbaev M, Laval J and Pommier Y (2004) Apoptotic topoisomerase I-DNA complexes induced by staurosporine-mediated oxygen radicals. *J Biol Chem* **279**(48):50499-50504.
- Staker BL, Feese MD, Cushman M, Pommier Y, Zembower D, Stewart L and Burgin AB (2005) Structures of three classes of anticancer agents bound to the human topoisomerase I-DNA covalent complex. *J Med Chem* **48**(7):2336-2345.
- Staker BL, Hjerrild K, Feese MD, Behnke CA, Burgin AB, Jr. and Stewart L (2002) The mechanism of topoisomerase I poisoning by a camptothecin analog. *Proc Natl Acad Sci U S A* **99**(24):15387-15392.
- Strumberg D, Pommier Y, Paull K, Jayaraman M, Nagafuji P and Cushman M (1999) Synthesis of cytotoxic indenoisoquinoline topoisomerase I poisons. *J Med Chem* **42**(3):446-457.
- Tewey KM, Chen GL, Nelson EM and Liu LF (1984) Intercalative antitumor drugs interfere with the breakage-reunion reaction of mammalian DNA topoisomerase II. *J Biol Chem* **259**(14):9182-9187.

Wall ME and Wani MC (1995) Camptothecin and taxol: discovery to clinic--thirteenth Bruce F. Cain Memorial Award Lecture. *Cancer Res* **55**(4):753-760.

Wang L, Price HL, Juusola J, Kline M and Phanstiel Ot (2001) Influence of polyamine architecture on the transport and topoisomerase II inhibitory properties of polyamine DNA-intercalator conjugates. *J Med Chem* **44**(22):3682-3691.

Wassermann K, Markovits J, Jaxel C, Capranico G, Kohn KW and Pommier Y (1990) Effects of morpholinyl doxorubicins, doxorubicin, and actinomycin D on mammalian DNA topoisomerases I and II. *Mol Pharmacol* **38**(1):38-45.

Xiao X, Antony S, Kohlhagen G, Pommier Y and Cushman M (2004) Design, synthesis, and biological evaluation of cytotoxic 11-aminoalkenylindenoisoquinoline and 11-diaminoalkenylindenoisoquinoline topoisomerase I inhibitors. *Bioorg Med Chem* **12**(19):5147-5160.

Xiao X, Miao ZH, Antony S, Pommier Y and Cushman M (2005) Dihydroindenoisoquinolines function as prodrugs of indenoisoquinolines. *Bioorg Med Chem Lett* **15**(11):2795-2798.

## FOOTNOTES

This research was supported (in part) by the Intramural Research Program of the NIH, National Cancer Institute, Center for Cancer Research. This project was funded in part with federal funds from the Developmental Therapeutics Program, Division of Cancer Treatment and Diagnosis, National Cancer Institute, National Institutes of Health, under contract NO1-CO-12400.

NCI-Frederick is accredited by AAALACi and follows the Public Health Service Policy on the Care and Use of Laboratory Animals. Animal care was provided in accordance with the procedures outlined in the Guide for Care and Use of Laboratory Animals (NIH publication No. 86-23, 1985).

This work was made possible by the National Institutes of Health (NIH) through support of this work with Research Grant UO1 CA89566 and Training Grant ST32 CA09634-12. This research was conducted in a facility constructed with support from Research Facilities Improvement Program Grant Number C06-14499 from the National Center for Research Resources of the NIH.

The content of this publication does not necessarily reflect the views or policies of the Department of Health and Human Services, nor does mention of trade names, commercial products, or organizations imply endorsement by the U.S. Government.

## FIGURE LEGENDS

**Fig. 1.** Chemical structures of the bisindenoisoquinoline NSC 727357, camptothecin (CPT) and the indenoisoquinolines NSC 725671 (monomer for the bisindenoisoquinoline), MJ-III-65 (NSC 706744) (Antony et al., 2003; Antony et al., 2005) and NSC 314622 (the parent indenoisoquinoline) (Kohlhagen et al., 1998). The dashed lines indicate the structural overlap seen in the crystal structure (Ioanoviciu et al., 2005; Marchand et al., 2006; Staker et al., 2005). The molecular weights for each of the compounds are: CPT, 348.4; NSC 314622, 365.34; NSC 706744, 452; NSC 725671, 340.8; and NSC 727357, 876.

**Fig. 2.** Proposed model for trapping of Top1 cleavage complexes by the bisindenoisoquinoline NSC 727357 and for inhibition of Top1 binding at high drug concentration. **A.** Top1 binds reversibly to DNA by forming Top1 cleavage complexes. These cleavage complexes are normally highly reversible and are hardly detectable under normal conditions. **B.** Camptothecins and indenoisoquinolines bind reversibly at the interface of the Top1-DNA cleavage complex (drug molecule shown as the black rectangle between the base pair at positions -1 and +1) (Ioanoviciu et al., 2005; Marchand et al., 2006; Staker et al., 2005; Staker et al., 2002). **C.** We propose that the bisindenoisoquinoline traps the Top1 cleavage complex by having one of the bisindenoisoquinoline aromatic rings bound at the interface of the Top1 cleavage complex while the other ring might bind externally to the DNA. **D.** Alternatively, the second aromatic ring might

be intercalated. **E.** At high concentrations, the bisindenoisoquinoline can prevent the binding of Top1 to DNA by saturating the DNA and/or specifically binding to the binding site of Top1 upstream from its potential cleavage site (Pommier et al., 2000).

**Fig. 3.** Top1-mediated DNA cleavage induced by NSC 727357.

**A,** The DNA corresponds to the 3'-end-labeled *PvuII/HindIII* fragment of pBluescript SK (-) phagemid DNA (pSK). DNA was reacted with Top1 in the absence of drug (Top1) or in the presence of 1  $\mu$ M CPT (CPT), 1  $\mu$ M NSC 706744 or the indicated concentrations ( $\mu$ M) of NSC 314622 and NSC 727357. Reactions were at 25°C for 20 min and stopped by adding 0.5% SDS. DNA fragments were separated in 16% denaturing polyacrylamide gels. **B,** Using the same DNA as in panel A, similar reactions were carried out with the indicated concentrations of NSC 725671 (monomer for NSC 727357). Numbers to the side of the gel indicate the migration positions of DNA fragments cleaved at these positions by Top1 in the pSK DNA. The base sequences encompassing the cleavage sites are represented, with the bases flanking the cleavage site highlighted in bold. Boxed sequences represent sites of Top1-mediated cleavage trapped by NSC 727357 and NSC 725671. **C,** The Top1-mediated cleavage products obtained upon drug treatment at site 92 from panel A were quantified relative to that obtained with Top1 alone and represented graphically.

**Fig. 4.** NSC 727357 unwinds DNA and inhibits Top1 catalytic activity at high

concentrations.

**A**, Native supercoiled  $\phi$ X174 DNA (supercoiled, Sc) (*lane 1*) was first reacted with excess Top1 to fully relax the DNA (relaxed, R) in the absence of drug (*lane 2*). Samples reacted with excess Top1 were then further incubated with the indicated concentrations of NSC 727357 (*lanes 3-9*) or in the absence of drug (*lane 10*) for 30 min at 37°C. Reactions were stopped with 0.5% SDS followed by 0.5 mg/ml proteinase K digestion and run in 1% agarose gel in TBE buffer containing 0.1% SDS. DNA was visualized after staining the gel with ethidium bromide. **B**, Similar reactions as in panel A were carried out with the indicated concentrations of NSC 725671 (*lanes 5-9*) and NSC 727357 samples (*lanes 3 & 4*, used for comparison). Sc, supercoiled DNA; R, relaxed DNA.

**Fig. 5.** Top2-mediated trapping by NSC 727357 at a selective site.

**A**, The pSK DNA fragment was the same as in Fig. 2 but labeled at the 5' end. Reactions were performed with Top2 in the presence of 100  $\mu$ M etoposide (VP-16) or the indicated concentrations ( $\mu$ M) of NSC 727357. After incubation at 25°C for 30 min, reactions were stopped by addition of 0.5% SDS. DNA fragments were then separated in a 16% denaturing polyacrylamide gel. **B**, A 38-mer oligonucleotide (sequence as shown in D) corresponding to the positions 1-38 (boxed in A) of the pSK DNA was generated and labeled at the 5'-terminus of either the upper strand (upper strand) or bottom strand (lower strand) followed by annealing to the unlabeled complementary strand. Labeled duplex

oligonucleotides were then subjected to the same treatments as in A with the indicated concentration ( $\mu\text{M}$ ) of drugs. **C**, The percent of Top2-mediated cleavage product obtained upon drug treatment from panel B were quantified and represented graphically. **D**, Sequence of the 38-bp oligonucleotide with the cleavage at site 17 on the upper strand indicated with a dashed arrow and the cleavage on the lower strand indicated with a solid arrow.

**Fig. 6.** NSC 727357 arrests cells in G1.

HT29 cells were treated in the absence (A) or presence of indicated concentrations ( $\mu\text{M}$ ) of NSC 727357 (B) or NSC 706744 (C) for 18 h. Fixed cells were stained with propidium iodide and analyzed for DNA content distribution histograms by flow cytometry.

**Fig. 7.** Short treatment with NSC 727357 does not inhibit thymidine incorporation.

**A**, Representation of the treatment schedule. **B**, HT29 cells were analyzed in the absence of drug (a & e) or immediately following treatment with either 1  $\mu\text{M}$  CPT (b) or 1  $\mu\text{M}$  (c) or 5  $\mu\text{M}$  (d) of NSC 727357 for 1 h. Cell cycle distribution and DNA synthesis were measured by BrdU labeling and PI staining. Cells pulse-labeled with 50  $\mu\text{M}$  BrdU (a-d) or without BrdU (e) for the last 30 min (as shown in panel A) were fixed, incubated with anti-BrdU antibody and PI and analyzed by flow cytometry. Scatter plots depict BrdU labeling (*y axis*, log scale) as a function of cell cycle distribution (*x axis*, PI content).

**Fig. 8.** Partial resistance of Top1-deficient and Top1-siRNA cells to NSC 727357. Growth inhibition in P388 wild type (—■—) and Top1-deficient (—○—), MCF-7 wild type (—■—) and Top1-siRNA (—○—) and HCT 116 wild type (—■—) and Top1-siRNA (—○—) cells was measured by MTT or SRB assay after treatment with varying concentrations ( $\mu\text{M}$ ) of NSC 727357 (A) or NSC 706744 (B) for 3 days. Percentage of growth of two independent experiments is represented as the mean  $\pm$  S.D.

**Fig. 9.** Partial resistance of p53-deficient cells to NSC 727357.

Cell survival of wt p53 (TK6, —■—) and p53 null (NH32, —○—) cells treated with camptothecin (panel A), NSC 706744 (panel B) and NSC 727357 (panel C) are represented. Cells were plated in sextuplicates in 96-well tissue culture plates and treated with drugs at indicated concentrations for 24 h. Cell survival was measured as described in Methods. One of two independent experiments is shown.

**Fig. 10.** Mean graph representation of the cytotoxicity profile of NSC 727357 in the 60 cell lines of the National Cancer Institute Anticancer Drug Screen. GI50s (the cytotoxicity GI50 values are the concentrations corresponding to 50% growth inhibition) were used to generate the graph. The profiles of CPT and NSC 706744 are shown for comparison. The mean GI50 across all the cell lines (*MG\_MID* or *MGM*; *mean graph midpoint*), the maximum difference from the

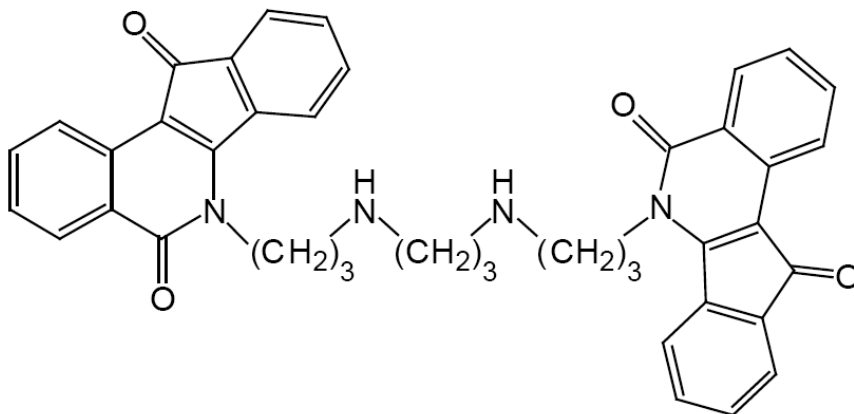


mean (Delta) and the difference between the highest and lowest values (Range) are indicated below each profile.

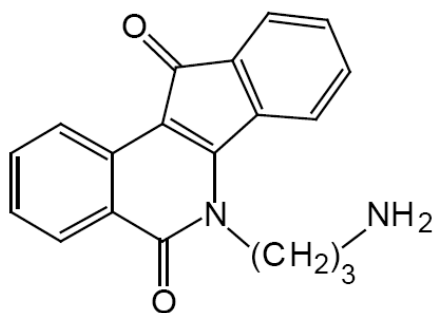
**Fig. 11.** NSC 727357 exhibits hollow fiber activity and antitumor activity against melanoma xenografts. **A**, Table representing the hollow fiber activity of NSC 727357 and Taxol (used for comparison). The IP (Intraperitoneal) and SC (Subcutaneous) scores are the combined scores of the two test doses listed. **B**, Antitumor activity of NSC 727357 against melanoma xenografts. Control (—■—), NSC 727357 13.4 mg/kg/dose by ip injection (—◇—), NSC 727357 20 mg/kg/dose by ip injection (—▲—), NSC 727357 30 mg/kg/dose by ip injection (—●—).

Figure 1

**NSC 727357**



**NSC 725671**

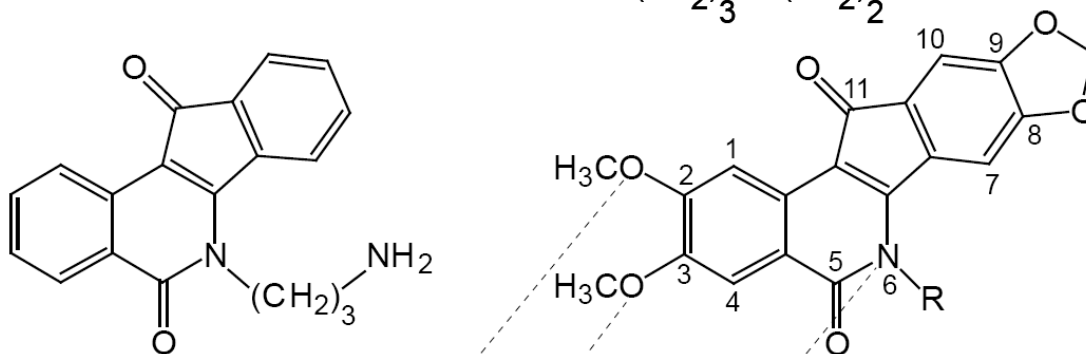


**NSC 314622**

R =  $\text{CH}_3$

**NSC 706744 (MJ-III-65)**

R =  $(\text{CH}_2)_3\text{NH}(\text{CH}_2)_2\text{OH}$



**CPT**

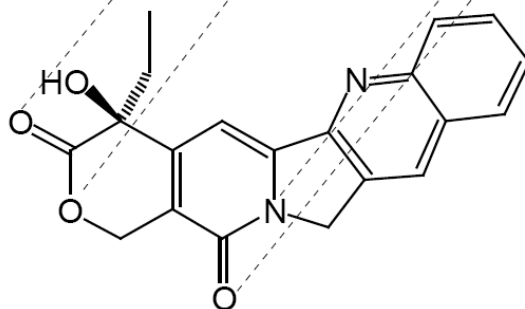


Figure 2

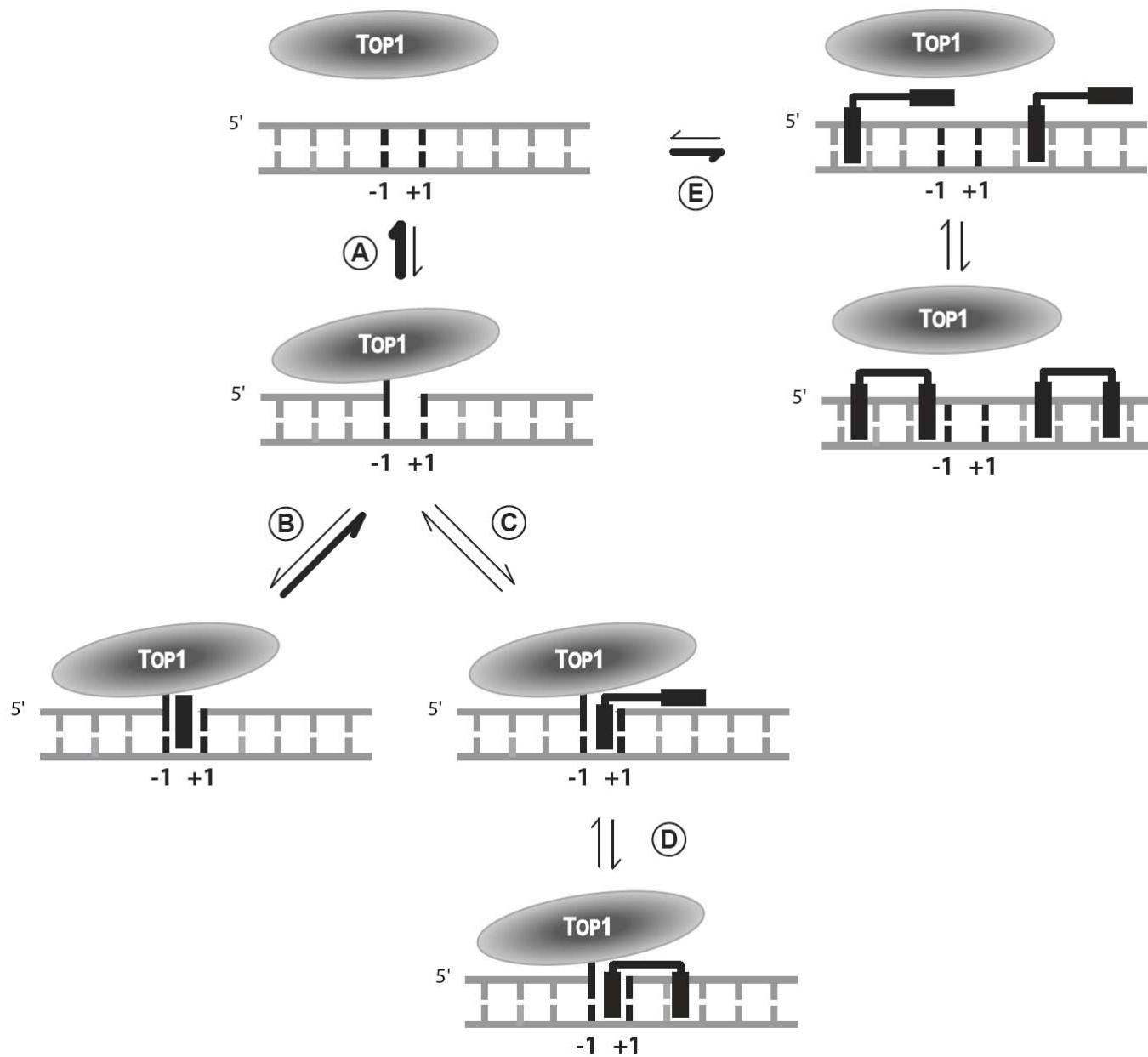


Figure 3

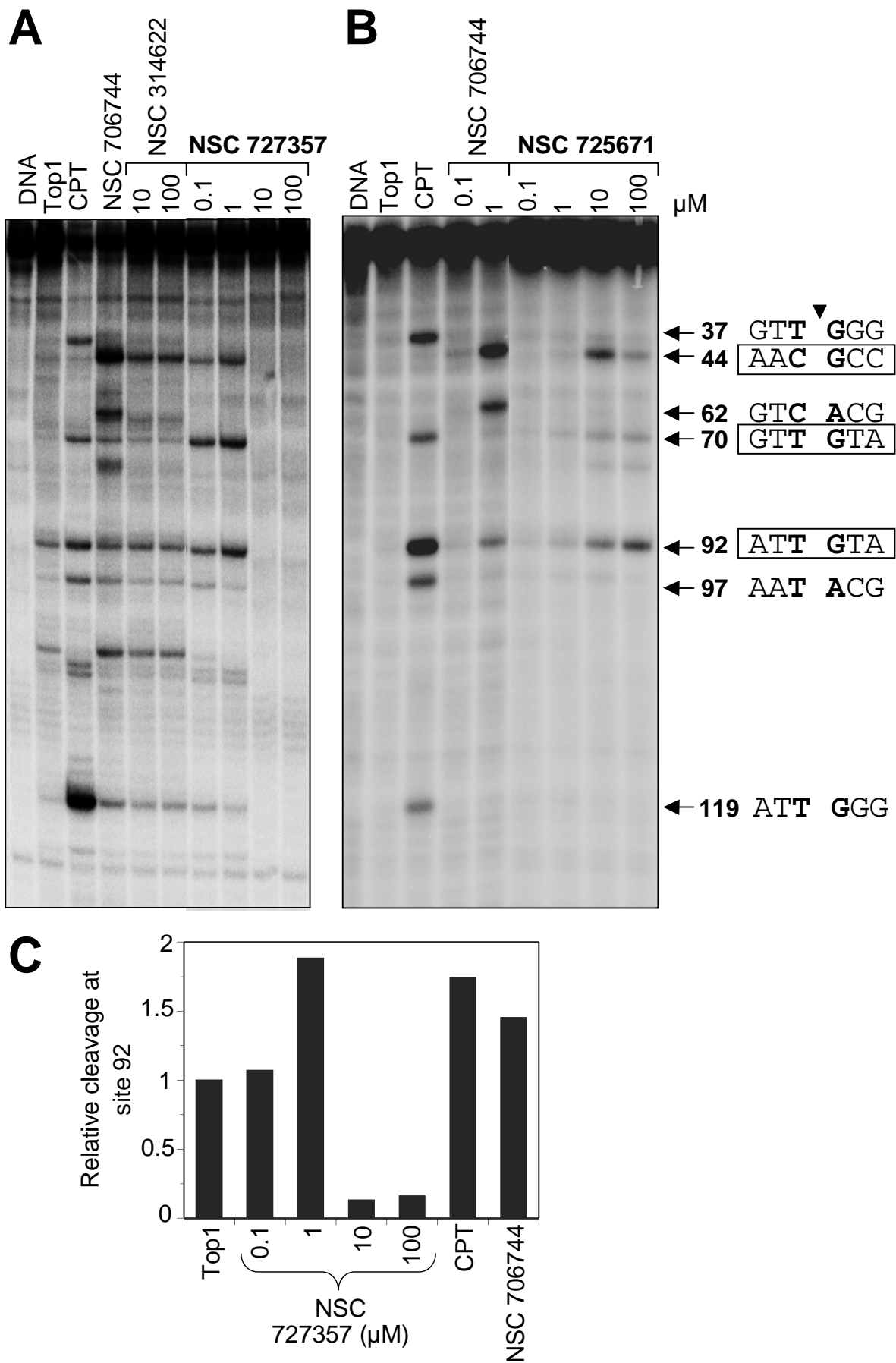
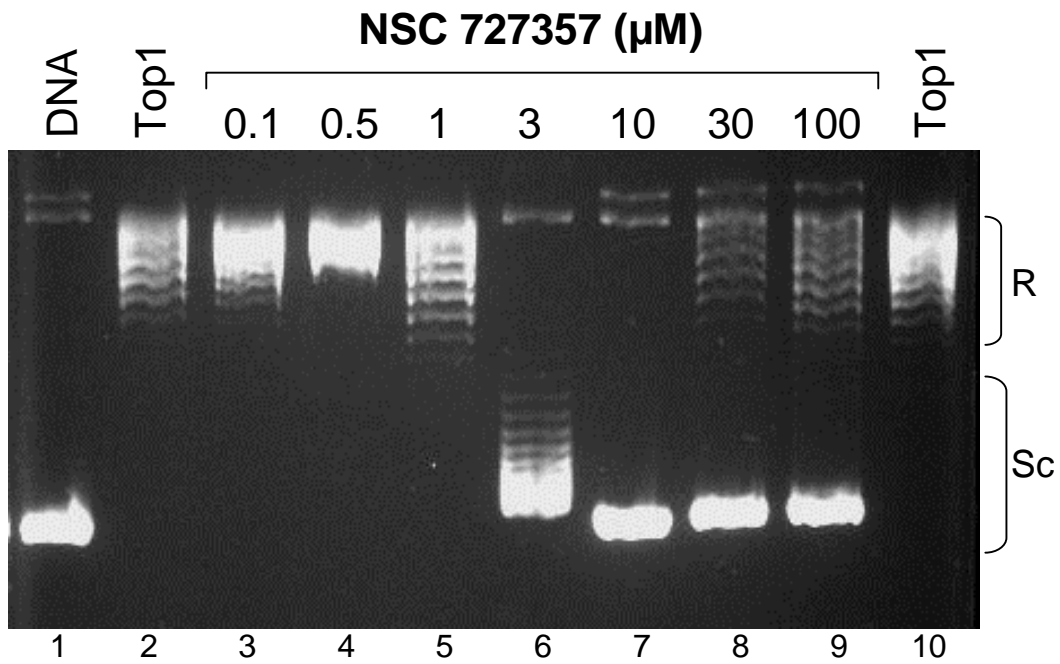


Figure 4

**A**



**B**

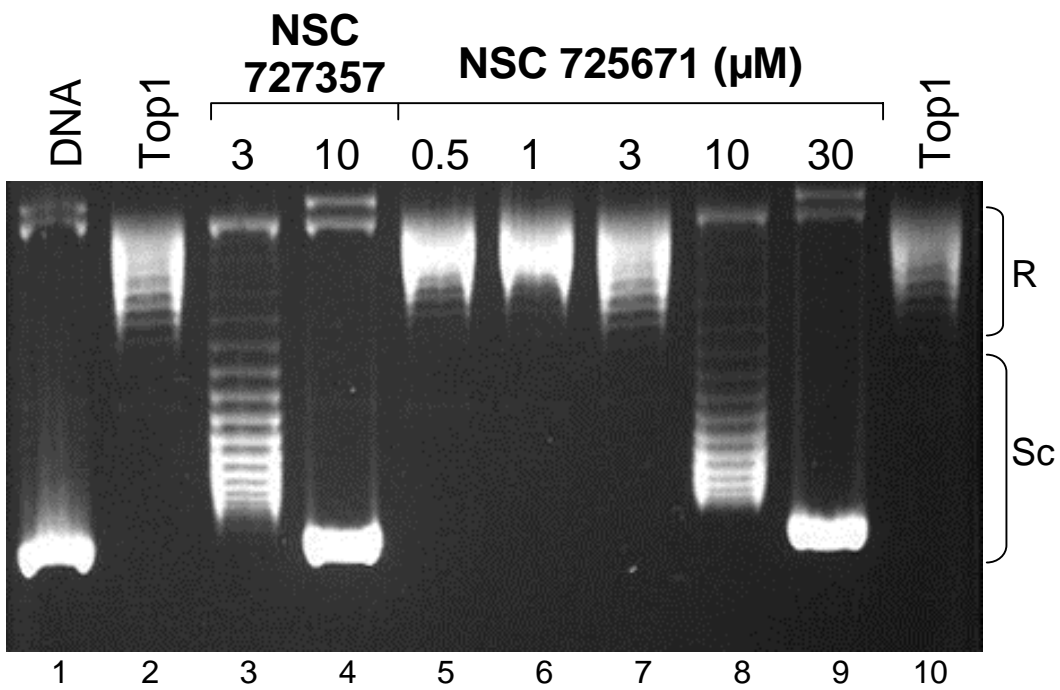


Figure 5

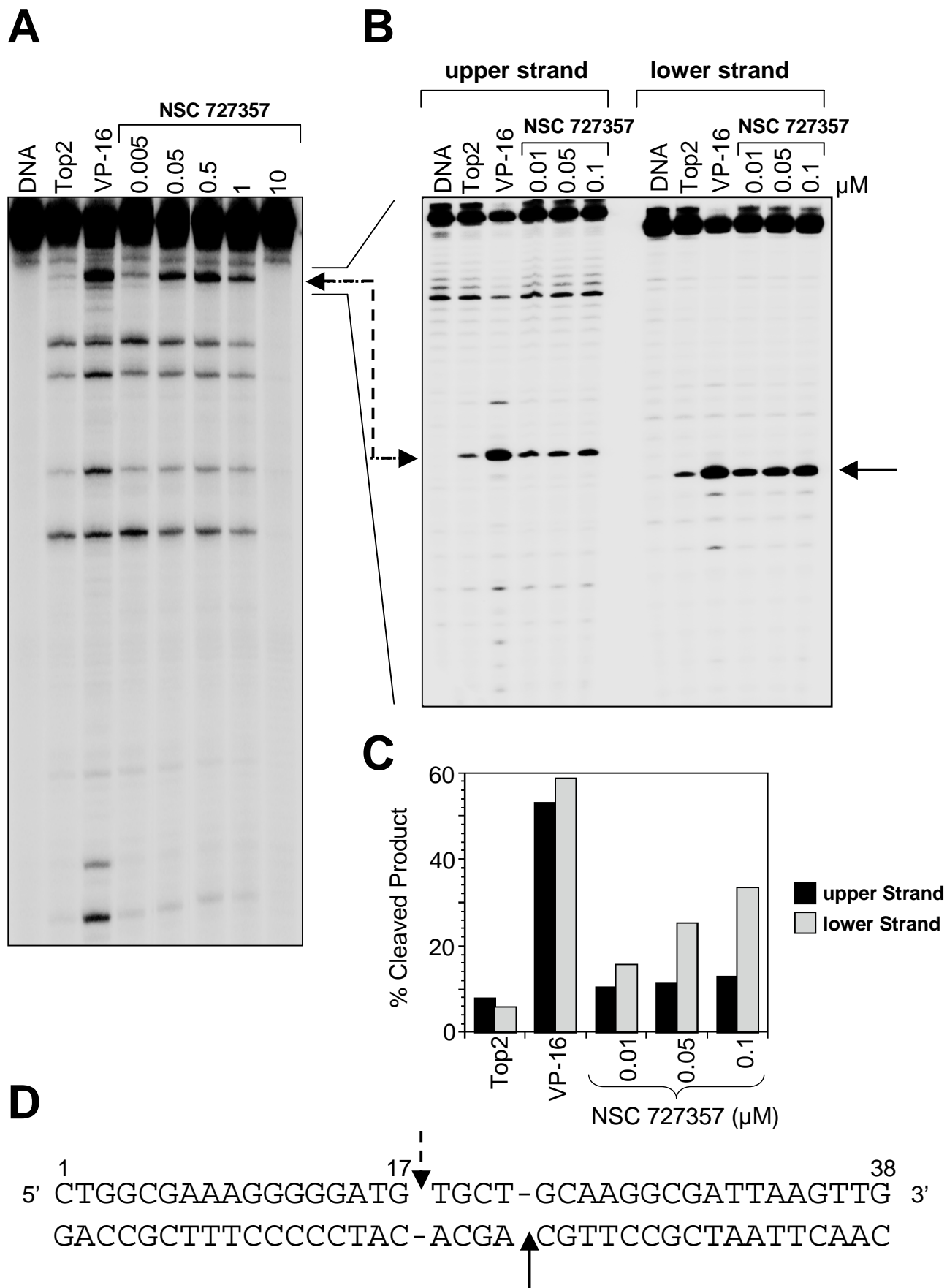


Figure 6

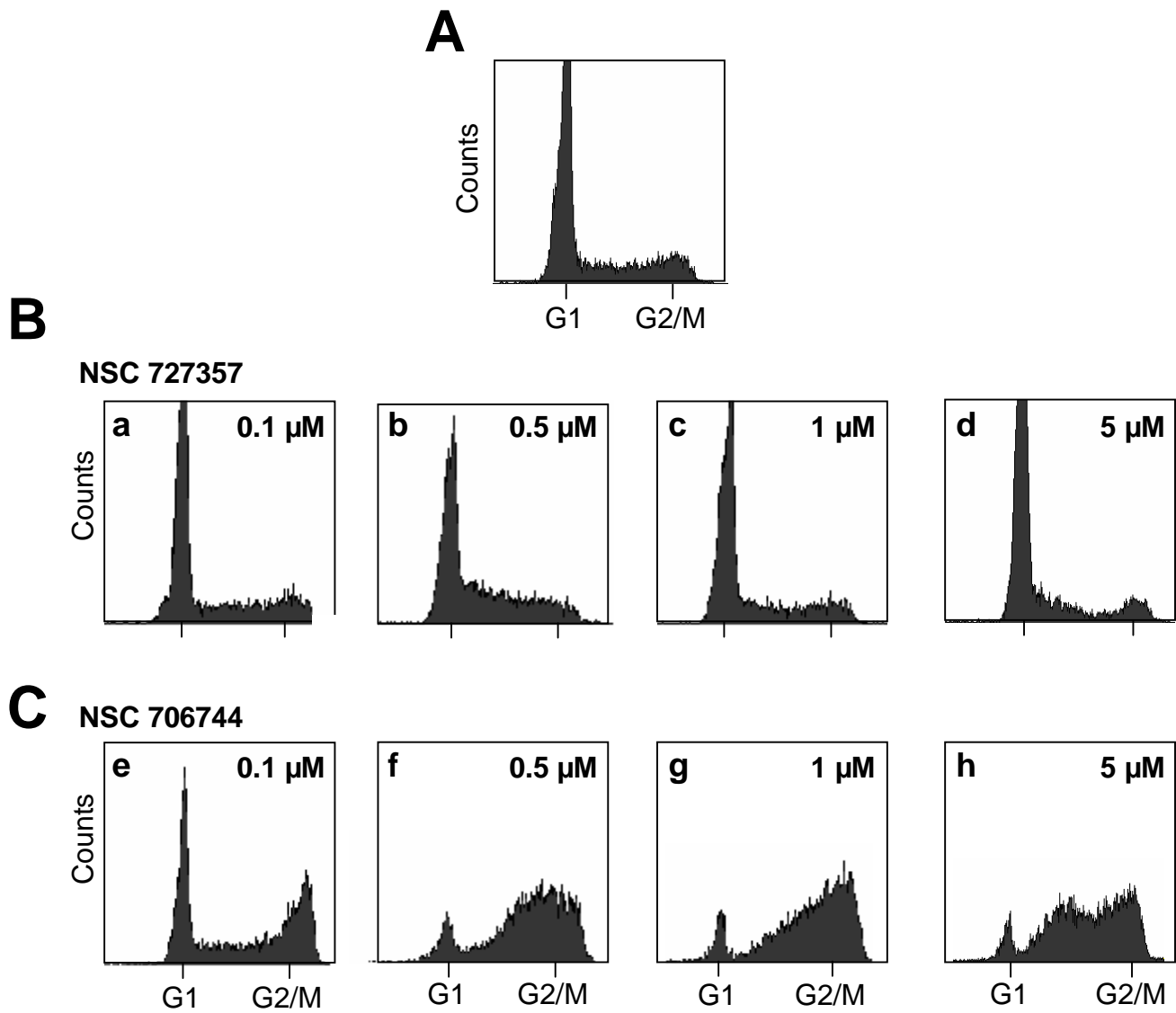


Figure 7

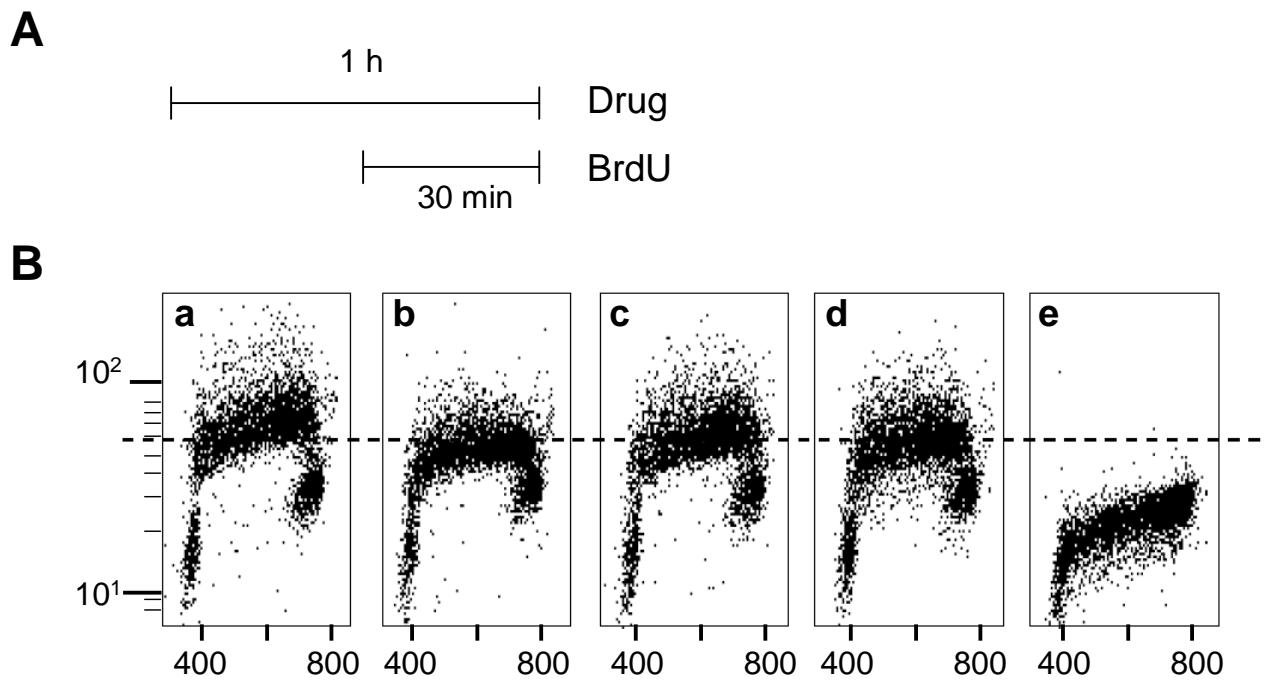




Figure 8

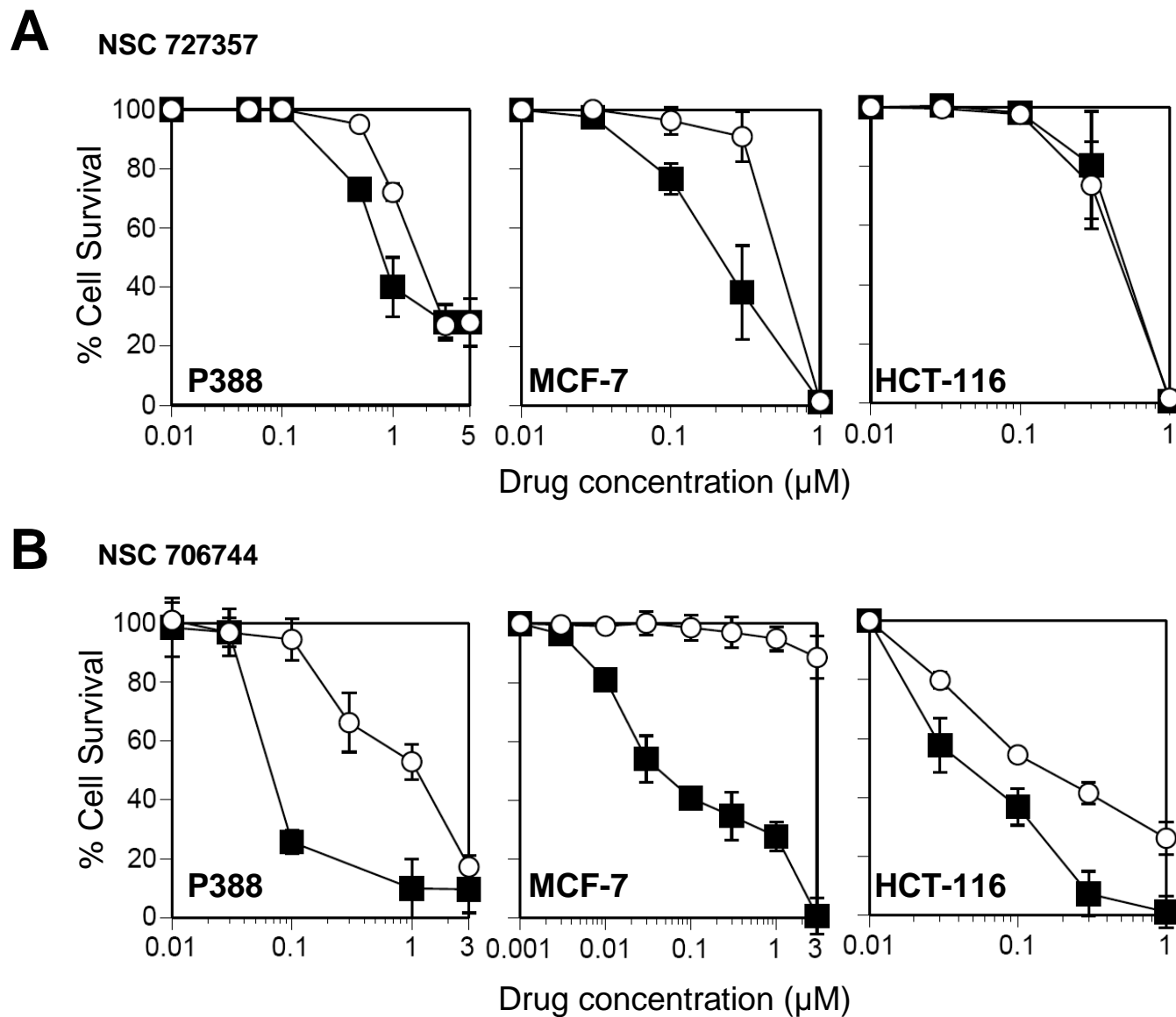


Figure 9

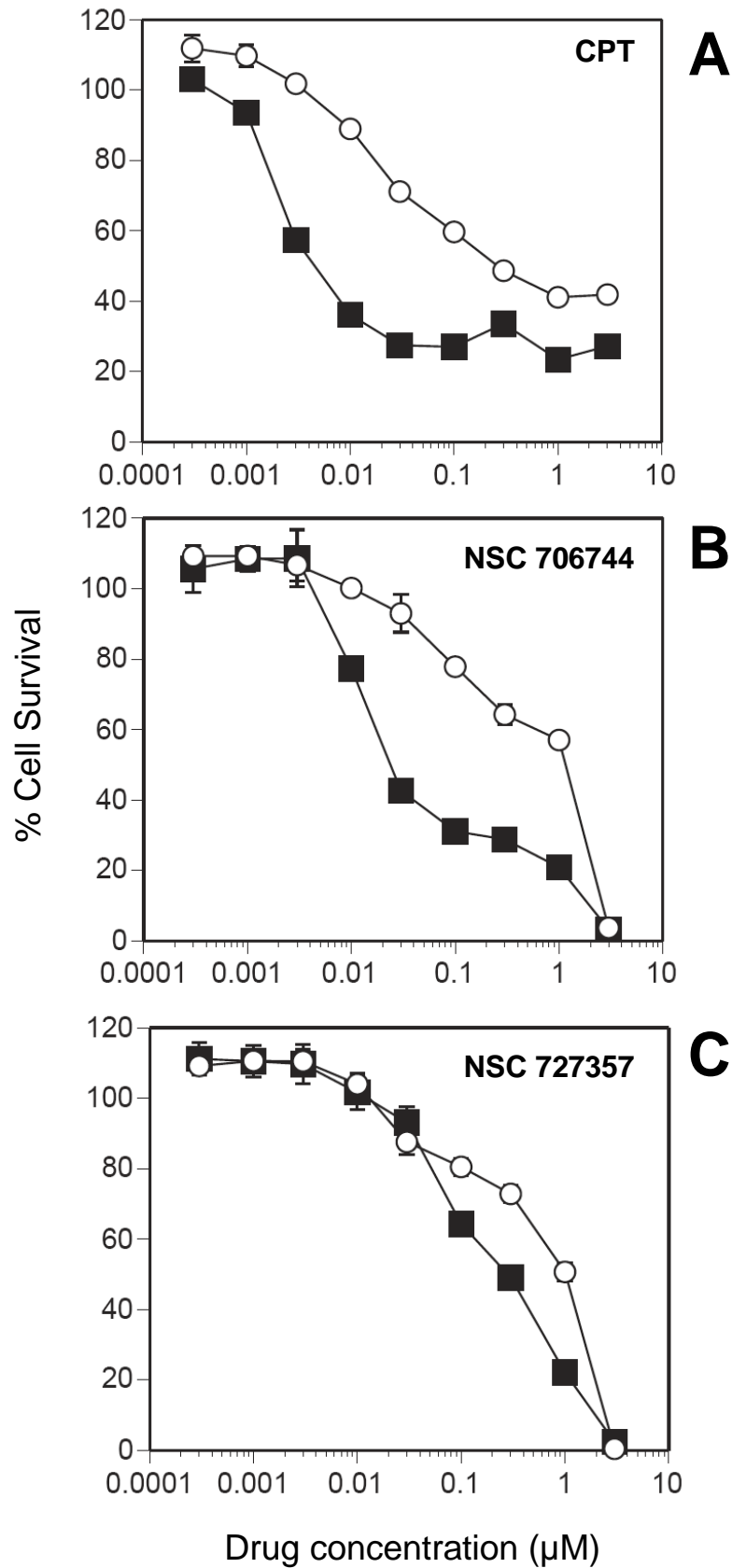


Figure 10

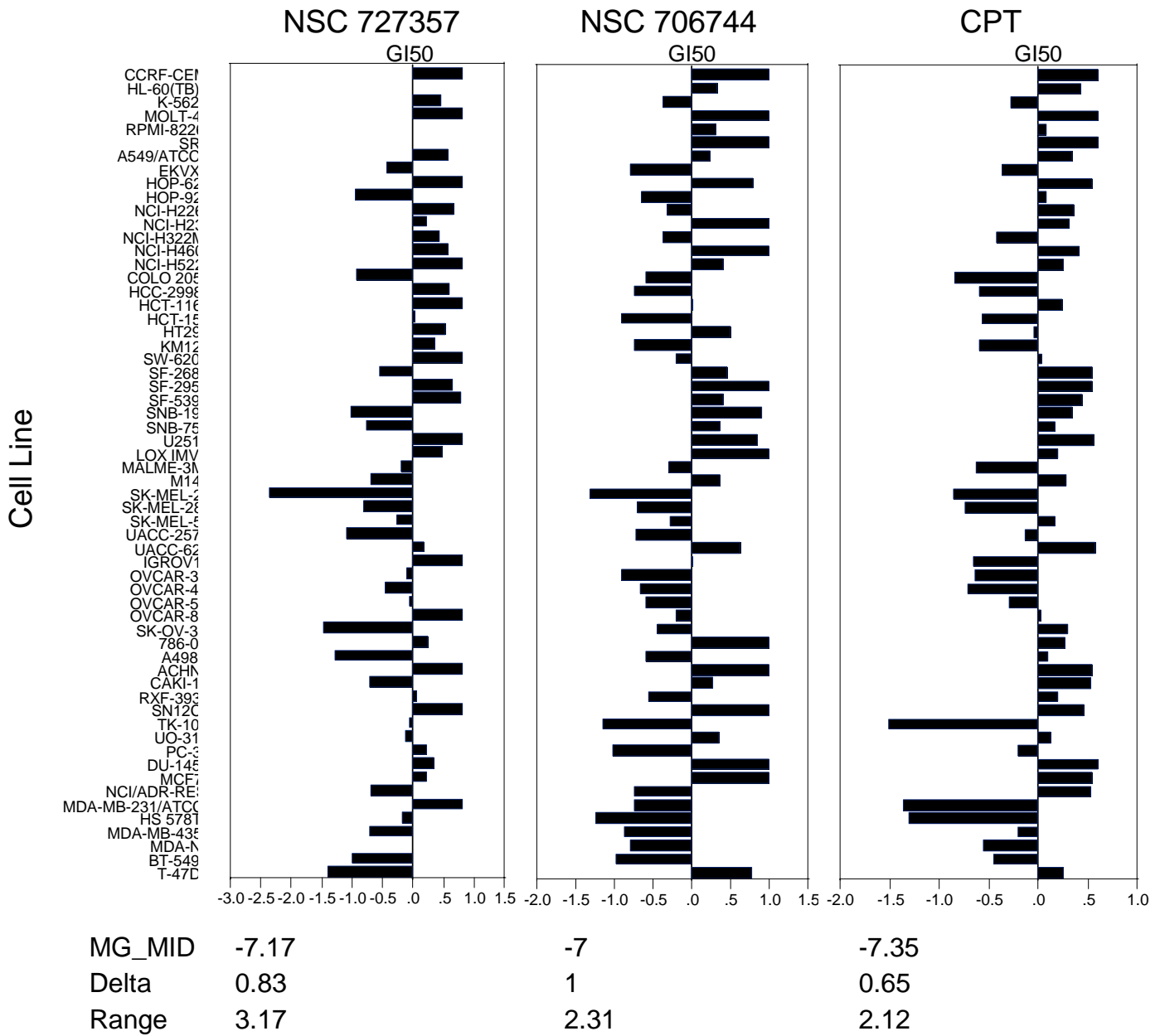


Figure 11

**A**

Drug	Test Doses (mg/kg)	IP Score	SC Score	Total Score
NSC 727357	30, 20	26	6	32
Taxol (NSC 125973)	15, 10	32	6	38

**B**

